

Impact of Dynamic Environmental Conditions on the Output Behaviour of Photovoltaics

Christian Schuss¹, Toni Kotikumpu¹, Bernd Eichberger², Timo Rahkonen¹

¹*Electronics Laboratory, University of Oulu, Erkki Koiso-Kanttilan katu 3, 90570 Oulu, Finland
christian.schuss@ee.oulu.fi, toni.kotikumpu@student.oulu.fi, timo.rahkonen@ee.oulu.fi*

²*Institute of Electronics, Graz University of Technology, Infieldgasse 12, 8010 Graz, Austria
bernd.eichberger@tugraz.at*

Abstract – This paper discusses the influences of dynamic environmental conditions on the output performances of photovoltaics. Commonly, photovoltaic (PV) modules are installed on the roofs of houses, onto which shading is caused by clouds and surrounding objects such as trees and other buildings. These ambient conditions can be referred as static environmental conditions. We also elaborate on the differences in the rate of change in the solar radiation level if PV modules are mounted onto the top of battery-powered electric vehicles (BEVs) and hybrid electric vehicles (HEVs). We present a comparison of static and dynamic environmental conditions which is helpful in evaluating the performance of maximum power point tracking (MPPT) techniques.



Fig. 1. Illustration of shading in a street.

I. INTRODUCTION

Solar energy is considered as one of the most promising renewable energy resources for the near future, especially for the substitution of energy gained from fossil fuels such as oil, coal and gas [1]. However, the opportunity to produce electricity with the help of photovoltaics directly is interesting for many different types of applications. For example, in wireless sensor network (WSN) nodes, the operating life time can be prolonged [2]. In terms of consumer electronics such as portable devices, solar energy as an additional power source is helpful in overcoming the limitation of battery capacity [3], [4].

The increasing popularity of photovoltaics brings them into many new types of environments. Normally, photovoltaic (PV) modules are installed on the roofs of houses. This fixed location for photovoltaics is referred to as a static environment for solar energy production. Here, shading can be caused by clouds as well as by surrounding objects such as trees and other buildings. Photovoltaics can be also deployed on the top of battery-powered electric vehicles (BEVs) and hybrid electric vehicles (HEVs) to extend the pure-electric driving distance and, in the case of HEVs, reduce fuel consumption [5], [6].

The situation when vehicles drive through urban and residential areas is referred as dynamical environmental con-

ditions. Here, alternation rates of ambient conditions differ from the ones in a static environment. It is crucial in this instance that the circumstances for photovoltaics in dynamic environmental conditions are studied in order to optimise strategies in order to gain the maximum amount of power from photovoltaics [6], [7]. Fig. 1 shows an example for shading in a street. Shadow on the roads depends on the location, the time of day and year, the driving direction, the size of the vehicle, and many other factors.

In the case of solar chargers for portable devices such as mobile phones, which can be mounted, for example onto bicycles or back bags, the ambient conditions of the bicycle lane/foot-walk on the left hand side of Fig. 1 are much better than the one on the right hand side. Unfortunately, the choice of the lane is not available for car drivers. Thus the question arises of how quickly the amount of sunlight changes when driving along the street and what impact the driving speed in general has on the output performance. In urban and residential areas, speed limits usually vary between 30 and 60 km/h.

II. BACKGROUND AND RELATED WORK

A. Output Behaviour of Photovoltaics

The I-V (Current-Voltage) curve illustrates the characteristic output behaviour of photovoltaics. The output

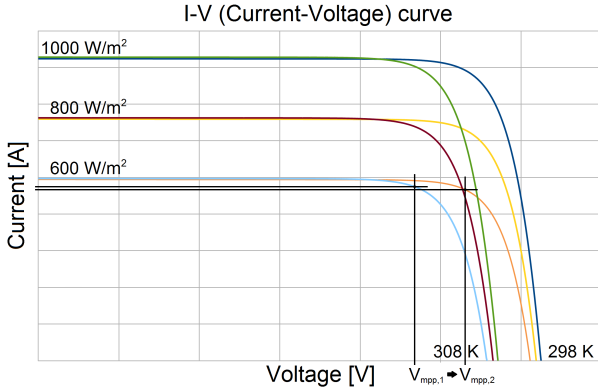


Fig. 2. I-V curve under different ambient conditions.

power level is strongly dependent on the solar radiation level (λ [W/m^2]) and varies with different temperatures of the PV cell (T_c [K]). Fig. 2 shows the variations in output performances of photovoltaics under different ambient conditions. As seen in Fig. 2, the position of the maximum power point (MPP) moves if the solar radiation level and temperature changes.

For example, if the solar radiation level is $600 \text{ W}/\text{m}^2$ and the PV cell temperature decreases by 10 K, the operating voltage (V_{op} [V]) needs to be altered from the previous voltage in the MPP ($V_{mpp,1}$ [V]) to the new voltage in the MPP ($V_{mpp,2}$ [V]). Hence, V_{op} needs to be continuously varied under changing environmental conditions towards the current V_{mpp} . For the design of the maximum power point tracking (MPPT) algorithm, it is important to have an understanding of the rate of change in environmental conditions.

B. Influence of Ambient Conditions on MPPT Techniques

In general, MPPT algorithms respond differently to fast changes in ambient conditions [7]. MPPT techniques also differ in other aspects from each other. Some MPPT algorithms do not consider the effects of aging of photovoltaics which causes a reduction of the open-circuit voltage (V_{oc} [V]) and short-circuit current (I_{sc} [A]) [7]. A classification of the different strategies can be established by factors such as:

- the complexity of the MPPT algorithm
- the structure of the power converter
- the parameters which are sensed
- the convergence speed
- the need of periodic tuning

However if, for example, the solar radiation changes quickly, some algorithms can cause failures; as shown in the example of the perturb and observe (P&O) algorithm,

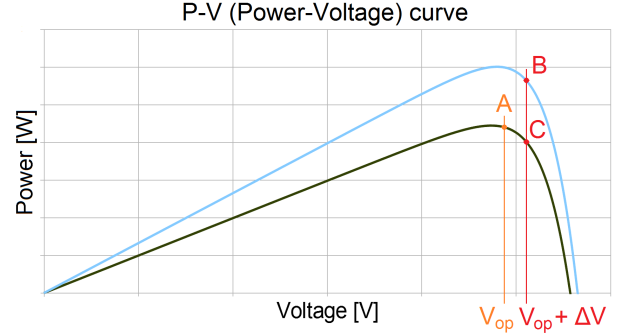


Fig. 3. Problem of the P&O algorithm.

illustrated in Fig. 3. At point A, a perturbation ΔV is made. If the ambient conditions change, the new operating point is B; if the ambient conditions remain constant, the result is point C. In point C, the correct decision is made and the perturbation is reversed due to the decreased power. At point B, the increase in power keeps the size and sign of perturbation the same. If the solar radiation increases continuously, the MPPT algorithm moves off the MPP based on incorrect assumptions [7].

C. Test Profiles for MPPT Algorithms

The rate of change in environmental conditions influences the performance of MPPT strategies. As mentioned before, MPPT is essential to ensure operating occurs at or close to the MPP. We define the alternation rate (r [$\frac{\text{W}}{\text{m}^2}/\text{sec}$]) to indicate the speed in which the amount of sunlight changes within a certain period of time. In this paper, we concentrate on the alternation rate of the solar radiation level (λ), obtained as follows:

$$r = \left. \frac{d\lambda}{dt} \right|_{\lambda_1}^{\lambda_2} \quad (1)$$

$$\begin{cases} \text{whereas } \lambda_2 > \lambda_1 & \text{for upward ramps} \\ \text{whereas } \lambda_2 < \lambda_1 & \text{for downward ramps} \end{cases}$$

Different test profiles are available in literature and allow for the evaluation of the performance of various MPPT techniques. Test protocols include slow and fast alternation rates as well as steady-state conditions [8]. Test sequences differ from each other, for example in the highest possible rate of change. r_{max} varies between 100 and 200 $\frac{\text{W}}{\text{m}^2}/\text{sec}$ [8], [9]. We will discuss if these values are suitable for static as well as for dynamic environmental conditions.

III. EVALUATION OF STATIC AND DYNAMIC ENVIRONMENTAL CONDITIONS

A. Static Environmental Conditions

Fig. 4 illustrates in a typical time frame of a partly cloudy, partly sunny day, in the city of Oulu, Finland dur-

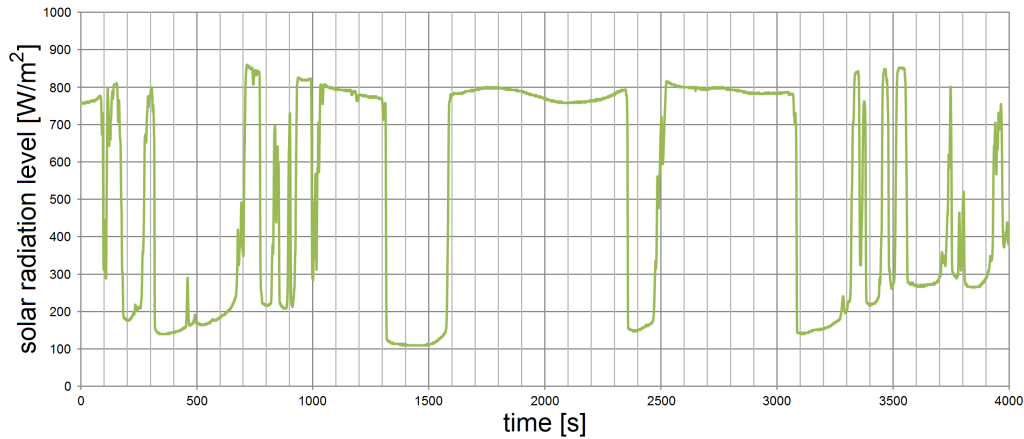


Fig. 4. Time frame of static environmental conditions.

ing the month of July. Data was collected at a sampling rate of 10 samples/sec. As seen in Fig. 4, after a longer period of time, cloud coverage broke up and for a few minutes the sun came out. Fast changes in ambient conditions were obtained, however, the alternation rate of the solar radiation level was often slow. In the case of a fixed installation of the measurement equipment, r_{max} was $253 \frac{W}{m^2}/sec$. This value fits reasonable well with the discussed test profiles for MPP trackers [8], [9].

B. Dynamic Environmental Conditions

In this investigation, four sensors were installed on the roof of a vehicle in order to measure the solar radiation level. The aim was to obtain the alternation rate during driving conditions in urban and residential areas. On streets, shading can be caused by many surrounding objects such as trees, lamp posts and buildings. The sensors were installed in the following locations: sensor 1 was placed at the front left corner, sensor 2 front right corner, sensor 3 rear left corner and sensor 4 rear right corner. The distance between each sensor (i.e between sensor 1 and 2) was about one metre. Data was collected at a sampling rate of 50 samples/sec.

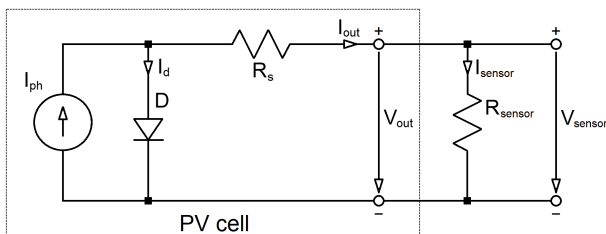


Fig. 5. Configuration of a solar radiation sensor.

Fig. 5 illustrates the configuration of one sensor which was used to measure the amount of sunlight and the alternation rate (r). Since the short-circuit current (I_{sc}) of a PV

cell is directly proportional to the solar radiation level (λ), a small resistor ($R_{sensor} [\Omega]$) was used to achieve a voltage ($V_{sensor} [V]$) which could be measured by the analog-to-digital converter (ADC) of a microcontroller unit (MCU). Here, it is crucial to stay within the linear region of the I-V curve and to operate as close to I_{sc} as possible.

It is worth noting that PV cells which are used as solar radiation sensors need to be characterised beforehand. I-V curves indicate the internal losses of PV cells. The accuracy of the measurement can be improved if PV cells with similar output characteristics are used. As mentioned above, one sensor was installed in each corner of the roof of a vehicle. Fig. 6 shows the measurement setup in which a MCU was present and collected data from each sensor. The system was calibrated with a Voltcraft PL-110SM solar radiation measuring instrument in order to calculate the amount of sunlight (in W/m^2) from the measured voltage drop over R_{sensor} (V_{sensor}).

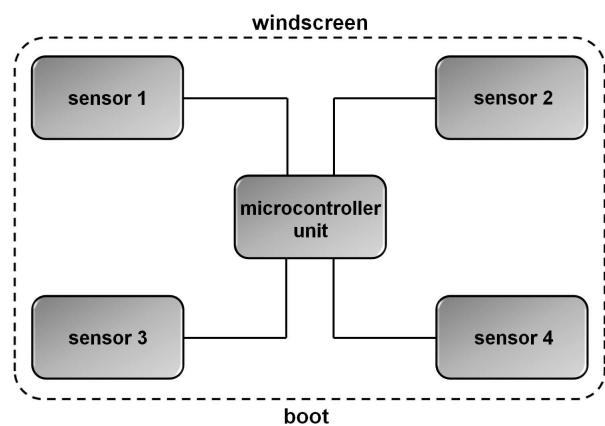


Fig. 6. Measurement setup on the roof of a vehicle.

Fig. 7 and Fig. 8 illustrates the measurements that were taken in the street, as shown in Fig. 1. At first, the vehicle with the four sensors was driving on the left-hand side

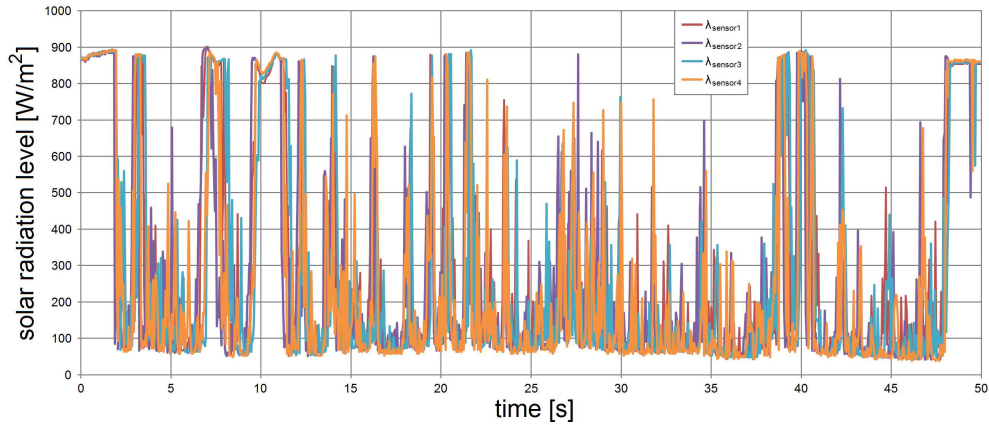


Fig. 7. Time frame of dynamic environmental conditions (measurement 1).

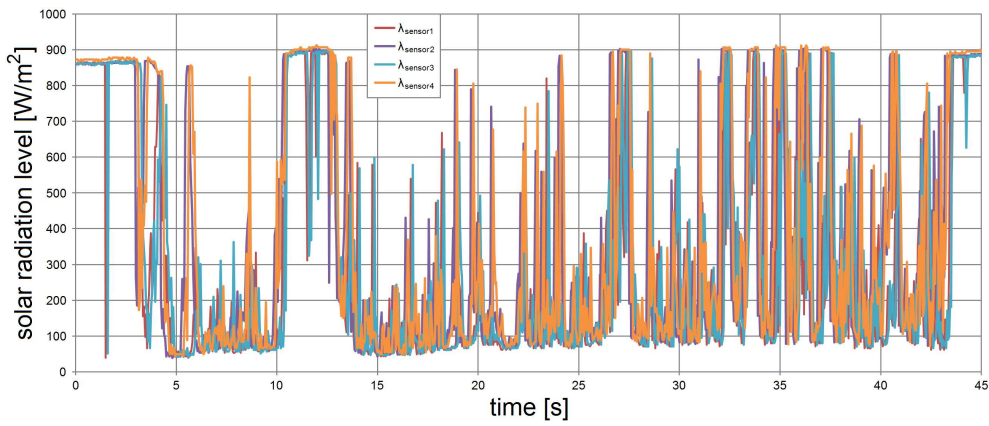


Fig. 8. Time frame of dynamic environmental conditions (measurement 2).

of the road (measurement 1) before crossing to the right-hand side (measurement 2). The speed of the vehicle was about 30 km/h. As seen in Fig. 1, there is more shadow present on the left-hand side compared to the right-side. Therefore, as expected, less sunlight will be obtained on this side of the street. In the presented measurement data, a small delay can be seen between the sensors in the front, close to the windscreen and those towards the rear, close to the boot.

As seen in Fig. 7 and Fig. 8, the solar radiation level is fluctuating, frequently changing from diffuse illumination to full sunlight. Here, r_{max} is as large as 332 W/m^2 in 20 ms ($16.6 \frac{\text{W}}{\text{m}^2}/\text{ms}$). At one point, for 1 second, a large variation in the amount of solar radiation is observed. Even though the roof of the vehicle is often shaded, there is still the opportunity to obtain more solar energy (on average about 300 W/m^2) than from the diffuse illumination which is about 100 W/m^2 .

For another measurement, the vehicle was driving under a highway bridge at 60 km/h (measurement 3). Each lane of the highway bridge was separated from each other, which resulted in a short period of sunlight between the

two lanes. Fig. 9 shows the data at this particular point. Underneath the bridge, no diffuse illumination is available and therefore, r_{max} is as large as 330 W/m^2 in 20 ms ($16.5 \frac{\text{W}}{\text{m}^2}/\text{ms}$). The obtained alternation rates are suitable for the evaluation of MPPT algorithms in order to verify the impact of the response time on the amount of output power.

The different amounts of solar radiation also influences the way PV modules are installed on top of vehicles. In our previous research, we discussed the negative impact of individual PV cells on the output performance of interconnections [5], [6]. In a series connection of PV cells, the output current is determined by the weakest PV cell or the PV cell with the lowest amount of sunlight. If a PV module is established from the front to the rear of the vehicle, the output power will be reduced during the moment sensors 1 and 2 obtain shadow until sensor 3 and 4 measures sunlight.

IV. EFFICIENCY OF MPPT ALGORITHMS

In this section, we present simulation results and evaluate the circumstances for MPPT algorithms in static and dynamic environmental conditions. Table 1 summarises

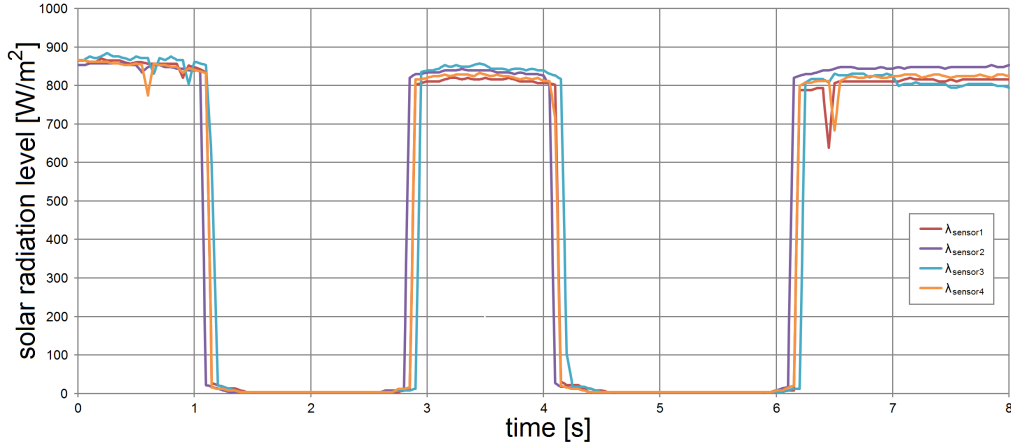


Fig. 9. Time frame of dynamic environmental conditions (measurement 3).

the parameters of the PV cell at standard test conditions (STC) which are used in the simulation tool to model photovoltaics and compute the performance of MPPT strategies [10]. In general, the degree of efficiency of MPPT techniques (η_{MPPT} [%]) can be obtained by comparing the output power (P_{out}) with the power in the MPP (P_{mpp}), as follows:

$$\eta_{MPPT} = \frac{\int_0^T P_{out}(t) dt}{\int_0^T P_{mpp}(t) dt} \quad (2)$$

Table 1. Parameters of a PV cell

Parameter	Value
P_{mpp} [W]	4.140
V_{mpp} [V]	0.515
I_{mpp} [A]	8.039
P_{th} [W]	5.273
V_{oc} [V]	0.613
I_{sc} [A]	8.602
FF	0.785

A. Voltage-based and Current-based MPPT

In voltage-based maximum power point tracking (VMPPT), the voltage in the MPP (V_{mpp}) is assumed as a fraction (M_V) of the open-circuit voltage (V_{oc}). Similarly, in current-based maximum power point tracking (CMPPT), the current in the MPP (I_{mpp}) is estimated as a fraction (M_I) of the short-circuit current (I_{sc}). Therefore, V_{oc} and I_{sc} are sensed periodically [7], [11]. In this paper, we focus on VMPPT by analysing the impact of different sampling rates of the V_{oc} in order to estimate the reduction in the efficiency of the algorithm. Fig. 10 and Fig. 11 illustrates the performance of VMPPT at different sampling rates in different environmental conditions.

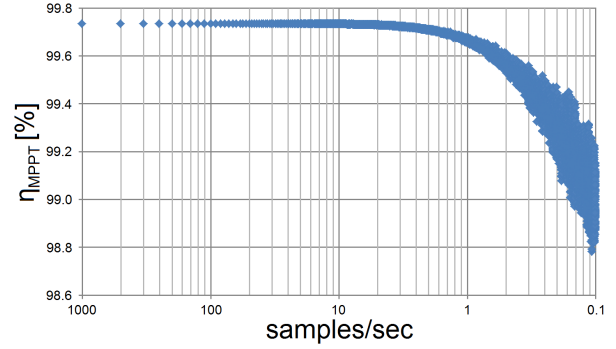


Fig. 10. Efficiency of VMPPT (static environment).

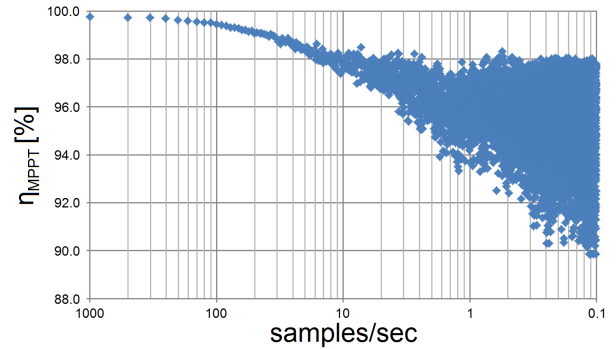


Fig. 11. Efficiency of VMPPT (dynamic environment).

$$\begin{aligned} \bar{\eta}_{MPPT} &= 98.94 \pm 0.23 \text{ W/m}^2 && \text{static environment} \\ \bar{\eta}_{MPPT} &= 94.62 \pm 1.41 \text{ W/m}^2 && \text{measurement 1} \\ \bar{\eta}_{MPPT} &= 95.12 \pm 1.51 \text{ W/m}^2 && \text{measurement 2} \\ \bar{\eta}_{MPPT} &= 87.63 \pm 12.05 \text{ W/m}^2 && \text{measurement 3} \end{aligned}$$

B. P&O Algorithm

As mentioned above, if ambient conditions change quickly, the operating point can move off the MPP. In the

simulation, the P&O algorithm coped better with situations like the highway bridge (measurement 3) than with shading conditions in streets (measurement 1 and 2). The reason for this is that in measurement 3 the solar radiation was constant for a few moments which allowed the P&O algorithm to recover. Furthermore, the efficiency is fluctuating which depends on the data.

V. DISCUSSION AND CONCLUSION

In this short article, we have elaborated upon the differences between static and dynamic environmental conditions for photovoltaics, whilst focusing on the alternation rate of ambient conditions such as the solar radiation level. Commonly, PV modules are installed on fixed locations and the rate of change depends on how quickly and how frequently clouds block the sunlight of the PV installation. We discussed the typical values for alternation rates which are used in test profiles for MPPT algorithms. Here, alternation rates lie commonly in the range of 100 and 200 $\frac{W}{m^2}/sec$.

Four sensors were installed on the roof of a vehicle to collect measurement data on the amount of sunlight during driving conditions. On streets and bicycle roads, shading is caused by surrounding objects such as buildings, lamp posts and trees. Ambient data also repeated this observation for one particular scenario in which the vehicle was driving under a highway bridge. It was shown that the rate of change is much higher under dynamic environmental conditions in comparison to static environmental conditions. The highest alternation rate was about 340 W/m^2 in 20 ms ($17 \frac{W}{m^2}/ms$).

It is worth noting that there are many strategies available when deciding which process is best to carry out MPPT. Even though the majority of solar energy will be obtained from the PV installation of a BEV or HEV under parking conditions, solar energy can also be gained under driving conditions. In dynamic environmental conditions, large step sizes of MPPT techniques can reduce the efficiency (η_{MPPT}) by up to 15 %.

ACKNOWLEDGMENT

We wish to thank Infotech Oulu for financially supporting this research.

REFERENCES

- [1] S. Pacala, and R. Socolow, "Stabilization wedges: Solving the climate problem for the next 50 years with current technologies", *Science*, vol. 305, 2004, pp. 968-972.
- [2] C. Alippi, and C. Galperti, "An Adaptive System for Optimal Solar Energy Harvesting in Wireless Sensor Network Nodes", *IEEE Transactions on Circuits and Systems I, Regular Papers*, vol. 55, issue: 6, 2008, pp. 1742-1750.
- [3] D. Jia, Y. Duan, and J. Liu, "Emerging technologies to power next generation mobile phone electronic devices using solar energy", *Frontiers of Energy and Power Engineering in China*, vol. 3, issue: 3, 2009, pp. 262-288.
- [4] C. Schuss, and T. Rahkonen, "Photovoltaic (PV) Energy as Recharge Source for Portable Devices such as Mobile Phones", *Proceedings of the 12th Conference of FRUCT Association*, 2012, pp. 120-128.
- [5] C. Schuss, B. Eichberger, and T. Rahkonen, "A Monitoring System for the Use of Solar Energy in Electric and Hybrid Electric Vehicles", *Proceedings of the IEEE International Instrumentation and Measurement Technology Conference (I2MTC)*, 2012, pp. 524-527.
- [6] C. Schuss, H. Gall, K. Eberhart, H. Illko, and B. Eichberger, "Alignment and Interconnection of Photovoltaics on Electric and Hybrid Electric Vehicles", *Proceedings of the IEEE International Instrumentation and Measurement Technology Conference (I2MTC)*, 2014, pp. 153-158.
- [7] T. Esrām, and P.L. Chapman, "Comparison of Photovoltaic Array Maximum Power Point Tracking Techniques", *IEEE Transactions on Energy Conversion*, vol. 22, 2007, pp. 439-449.
- [8] M. Ropp, J. Cale, M. Mills-Price, M. Scharf, and S.G. Hummel, "A test protocol to enable comparative evaluation of maximum power point trackers under both static and dynamic irradiance", *37th IEEE Photovoltaic Specialists Conference (PVSC)*, article number 6185961, 2011, pp. 3734-3737.
- [9] R. Bründlinger, N. Henze, H. Häberlin, B. Burger, A. Bergmann, and F. Baumgartner, "prEN 50530 - the new European Standard for Performance Characterization of PV Inverters", *24th European Photovoltaic Solar Energy Conference 2009*. [Online]. Available: http://labs.ti.bfh.ch/fileadmin/user_upload/lab1/pv/publikationen/4EP.1.2_EUPVSEC_Paper_EN50530_PV_inverter_Performance_-final-_090924.pdf
- [10] C. Schuss, and T. Rahkonen, "Adaptive Photovoltaic Cell Simulation with Maximum Power Point Tracking Simulation for Accurate Energy Predictions", *NORCHIP 2011*, article number 6126721, 2011, pp. 1-4.
- [11] M.A.S. Masoum, H. Dehbonei, and E.F. Fuchs, "Theoretical and Experimental Analyses of Photovoltaic Systems With Voltage- and Current-Based Maximum Power-Point Tracking", *IEEE Transactions on Energy Conversion*, vol. 17, issue: 4, 2002, pp. 514-522.